Electronic Supplementary Material (ESI) for Sustainable Energy & Fuels.

Supporting Information

The Oxygen Reduction Reaction Catalyzed by *Synechocystis 6803* Flavodiiron Proteins

Katherine A. Brown[a], Zhanjun Guo[a], Monika Tokmina-Lukaszewska[b], Liam W. Scott[b], Carolyn E. Lubner[a], Sharon Smolinski[a], David W. Mulder[a], Brian Bothner[b], and Paul W. King[a*]

[a]National Renewable Energy Laboratory, Golden, Colorado, USA
[b]Department of Chemistry and Biochemistry, Montana State University, Bozeman, Montana USA.

*To whom correspondence should be addressed:
National Renewable Energy Laboratory, Golden, Colorado, USA 80402;
email: Paul.King@nrel.gov Tel: 303 384-6277; Fax: 303 384-7836.

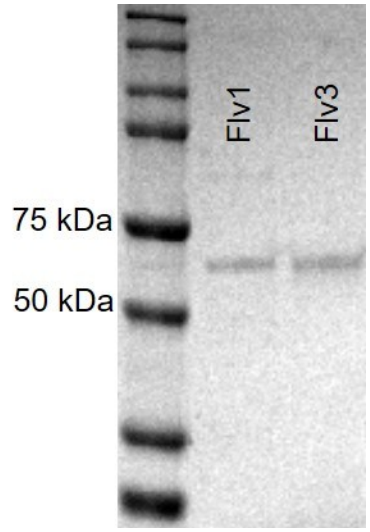

Figure S1. SDS-PAGE of purified Flv1 and Flv3. Calculated mass of monomer of Flv1 = 66.6 kDa; Flv3 = 65.1 kDa. Protein ladder shown in the left lane with 50 and 75 kDa molecular weight standards labeled.

Table S1. Reconstituted Flv1 and Flv3 flavin and iron content.

Flv	Absorbance 460 nm	Flavin concentration (μM)	Flv concentration (μM)	Flavin per- monomer[a]	Fe atoms per-monomer[a]
1	0.0550	5.6 ± 0.1	2. 9 ± 0.1	1.9 ± 0.11	1.9 ± 0.2
3	0.0710	7.2 ± 0.1	3.9 ± 0.1	1.8 ± 0.13	1.8 ± 0.2

[a]Values are ± SEM.

Table S2. FAD/FMN ratios for reconstituted Flv1 and Flv3 determined by phosphodiesterase (PDE) assay.

Sample	Fluorescence @ 520 nm	Fluorescence Ratio (enzyme/enzyme + PDE)	Flavin ratio (FAD/FMN)[a]
Flv1	9226	3.08 ± 0.05	3.0 ± 0.1
Flv1 + PDE	28413		
Flv3	50743	1.25 ± 0.05	0.3 ± 0.06
Flv3 + PDE	63510		

[a]FAD, flavin adenine dinucleotide; FMN, flavin mononucleotide (± SEM).

Table S3. Hill kinetics of Flv1 and Flv3 NAD(P)H oxidation under atmospheric O_2[a].

Flv	Reduced Pyridine Nucleotide	K'[a]	V_{max}[b]	k_{cat} (s^{-1})	n[b]	k_{cat}/K' (M^{-1} s^{-1})[c]
1	NADH	103 ± 10	43 ± 3	47	2.3 ± 0.6	4.5 x 10^5
	NADPH	114 ± 30	24 ± 4	25	1.6 ± 0.1	2.2 x 10^5
3	NADH	124 ± 28	26 ± 4	26	1.8 ± 0.5	2.1 x 10^5
	NADPH	128 ± 40	30 ± 6	32	1.6 ± 0.4	2.5 x 10^5

[a]Values of K' (reduced pyridine nucleotide, μM) were obtained from fits to the steady-state Hill equation, $v = V_{max}\left(\frac{[S]^n}{K' + [S]^n}\right)$ in reactions with 223 μM O_2 (± SEM). The individual rate values are shown in Table S3.
[b]μmol NAD(P)H mg^{-1} min^{-1} (± SEM). Hill coefficient (n) for NAD(P)H (± SEM).
[c]per-monomer (± SEM).

Table S4. O_2-dependent NAD(P)H oxidation rates by Flv1 and Flv3.

NAD(P)H (μM)[a]	Flv1[b]		Flv3[d]	
	V_{NADH} (μmol NADH mg Flv1^{-1} min^{-1})[c]	V_{NADPH} (μmol NADPH mg Flv1^{-1} min^{-1})[c]	V_{NADH} (μmol NADH mg Flv1^{-1} min^{-1})[c]	V_{NADPH} (μmol NADPH mg Flv1^{-1} min^{-1})[c]
22	4.0 ± 0.3	3.0 ± 0.4	2.6 ± 0.3	3.6 ± 0.4
45	7.7 ± 0.8	3.6 ± 0.6	4.9 ± 0.4	5.1 ± 0.3
68	10.8 ± 0.9	3.7 ± 1.1	6.3 ± 0.9	7.7 ± 0.4
95	13.7 ± 1.3	8.9 ± 2.0	9.6 ± 1.8	10.8 ± 1.6
128	22.3 ± 3.1	11.2 ± 2.5	13.4 ± 2.2	16.3 ± 1.5
170	38.5 ± 1.5	16.1 ± 0.7	17.4 ± 1.0	19.2 ± 1.9
240	41.3 ± 1.6	16.7 ± 2.4	22.7 ± 1.1	22.5 ± 1.5
292	42.4 ± 1.3	17.8 ± 2.3	20.9 ± 1.5	23.8 ± 1.7
326	36.2 ± 2.5	19.8 ± 1.8	20.2 ± 1.0	23.5 ± 2.1

[a]223 μM O_2, 5% glycerol, 50 mM MOPS, pH 7.
[b]5 nM Flv1
[c]error calculated as standard deviation of N = 4 measurements
[b]5 nM Flv3

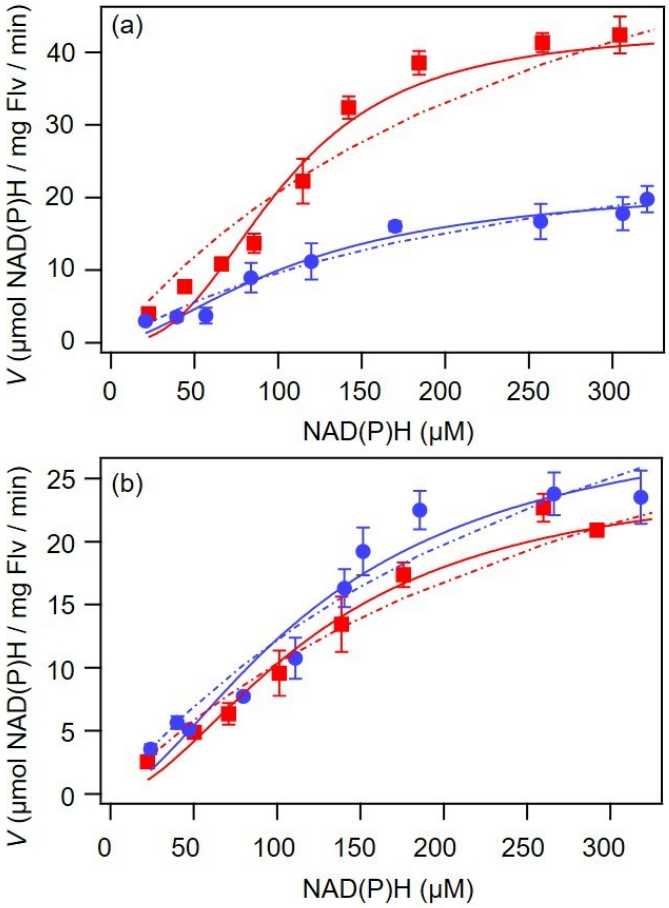

Figure S2. NAD(P)H oxidation kinetics by Flv1 (a) and Flv3 (b). Solid lines indicate fits of the steady state Hill equation, $v = V_{max}\left(\frac{[S]^n}{K' + [S]^n}\right)$. Dashed lines are fits to steady-state Michaelis-Menten equation $v = V_{max}\left(\frac{[S]}{K' + [S]}\right)$. Reactions were performed with 2.5 nM Flv and 223 µM O_2 in 5% glycerol, 50 mM MOPS, pH 7.

Table S5. Sum of Squared Residuals[a] for Hill and Michaelis-Menten fits of NAD(P)H oxidation kinetics.

Reduced Pyridine Nucleotide	Flv	Hill Equation Sum of Squared Residuals	Michaelis-Menten Equation Sum of Squared Residuals
NADH	1	80.7	191
	3	13.5	29
NADPH	1	9.5	23
	3	30	41

[a] $\sum_{i=1}^{n}((y_i - f(x_i))^2$; y_i = observed data for a [substrate]$_i$; $f(x_i)$ = value for [substrate]$_i$ calculated from fit values.

Table S6. NAD(P)H-dependent ORR rates for Flv1 and Flv3.

O_2 Concentration (μM)	Flv1[a]		Flv3[d]	
	V_{ORR} with NADH[b] (μmol O_2 mg $Flv1^{-1}$ min^{-1})[c]	V_{ORR} with NADPH[b] (μmol O_2 mg $Flv1^{-1}$ min^{-1})[c]	V_{ORR} with NADH[b] (μmol O_2 mg $Flv3^{-1}$ min^{-1})[c]	V_{ORR} with NADPH[b] (μmol O_2 mg $Flv3^{-1}$ min^{-1})[c]
35	5.9 ± 0.5	6.8 ± 0.8	2.5 ± 0.8	2.6 ± 1.3
107	9.3 ± 0.5	9.4 ± 1.1	7.5 ± 0.7	4.1 ± 1.1
142	16.7 ± 0.6	12.6 ± 0.7	8.6 ± 0.8	8.6 ± 0.7
223	25.4 ± 0.7	16.2 ± 0.9	16.6 ± 1.2	15.1 ± 1.6
335	39.4 ± 1.8	27.5 ± 1.8	24.0 ± 1.5	21.7 ± 0.6
448	33.0 ± 2.1	28.4 ± 2.1	26.5 ± 1.4	25.7 ± 0.9
778	33.8 ± 1.3	27.4 ± 1.3	26.5 ± 2.1	29.0 ± 2.4
1066	33.8 ± 1.6	27.4 ± 1.6	26.4 ± 1.7	27.5 ± 1.8

[a]12.5 nM Flv1
[b]1 mM NAD(P)H, 5% glycerol, 50 mM MOPS, pH 7
[c]error calculated as average error of N = 2 measurements
[d]12.5 nM Flv3

Table S7. Sum of Squared Residuals[a] for Hill and Michaelis-Menten fits of ORR reaction kinetics.

Reduced Pyridine Nucleotide	Flv	Hill Equation Sum of Squared Residuals	Michaelis-Menten Equation Sum of Squared Residuals
NADH	1	34	157
	3	31	70
NADPH	1	13	63
	3	9	57

Table S8. Rates of Flv1 and Flv3 catalyzed NAD(P)H oxidation and O_2 reduction in O_2 saturated solution.

Reduced Pyridine Nucleotide	**Flv**	$V_{NAD(P)H}$[a] **(µmol mg^{-1} min^{-1})**	V_{ORR}[b] **(µmol mg^{-1} min^{-1})**
NADH	1	72.1 ± 1.6	34.7 ± 1.6
	3	56.7 ± 2.2	26.4 ± 2.5
NADPH	1	66.7 ± 0.7	27.8 ± 2.1
	3	57.2 ± 1.5	31.5 ± 1.0

[a]Rate of NAD(P)H oxidation with 320 µM NAD(P)H and 1066 µM O_2 (± SEM).

[b]Rate of ORR with 1 mM NAD(P)H and 1066 µM O_2 (± SEM).

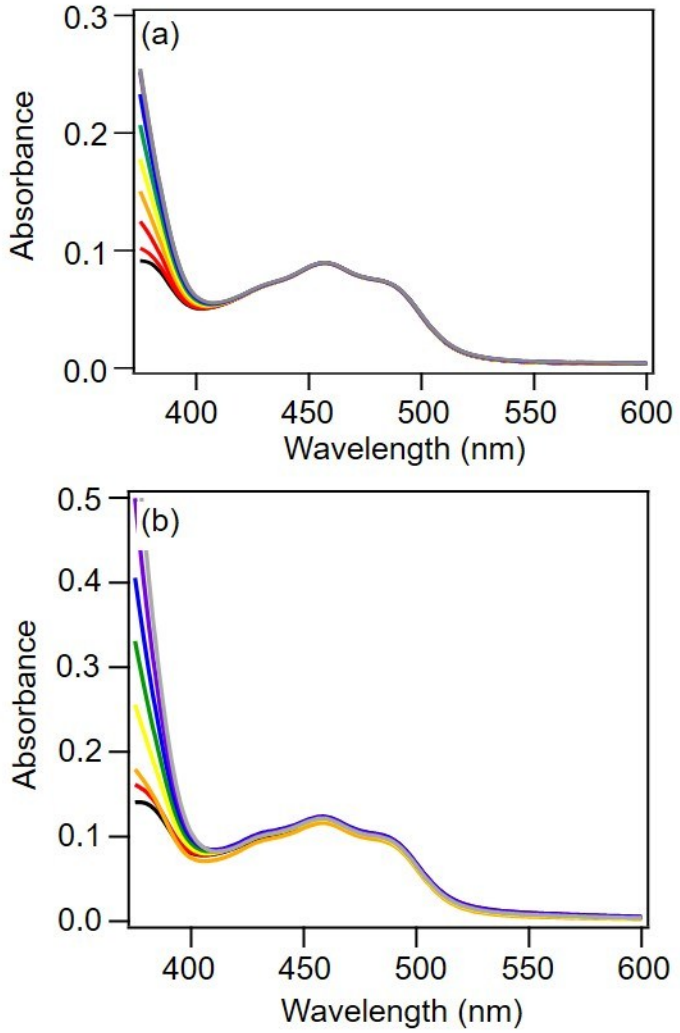

Figure S3. UV-Visible spectroscopy of Flv3 treated with NADPH (top) ord NADH (bottom) under O_2. Molar ratios of NAD(P)H:Flv3 are 0:1 (black line), 2:1 (red line), 4:1 (orange line), 6:1 (yellow line), 8:1 (green line), 10:1 (blue line), 12:1 (purple line), 14:1 (grey line). Reactions were performed with 25 µM Flv3 in 50 mM MOPS, 5% glycerol, 223 µM O_2, pH 7.

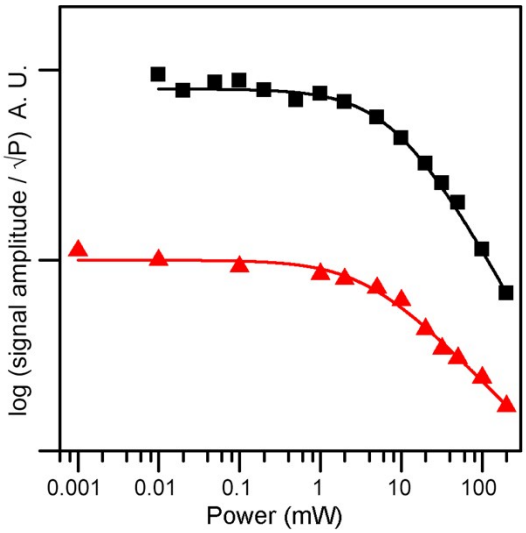

Figure S4. Power saturation curves for diiron (black) and radical (red) EPR signals observed from Flv3 reduced with NAD(P)H. The diiron signal (g = 1.93, 1.79, 1.70) amplitude was determined by double integration of the area, while the radical signal (g = 2) was determined by the peak to peak height. Both signals were measured at 5K and for microwave powers (P) ranging from 0.001 mW to 200 mW at a microwave frequency 9.38 GHz, modulation frequency 100 KHz, and modulation amplitude 10 Gauss. The half power of saturation ($P_{½}$) was determined to be 8.7 ± 1.9 and 3.6 ± 1.1 for the diiron and radical signals, respectively, by fitting to the equation y = log(A)-0.5*b*log(1+(x/c)) where A is the y offset, b is an inhomogeneity constant, x is the microwave power, and c is $P_{½}$.[1]

Figure S5. Complete data on surface labeling of intact Flv3 homodimer. Blue (DnsCl) and red (GEE) colored residues denote locations of incorporation, respectively, that were incorporated into the complex during short reactions (<10 mins for DnsCl and < 5 mins for GEE). Residues colored green represent where DnsCl/GEE labels were incorporated after longer reaction times, 15 and 10 minutes respectively.

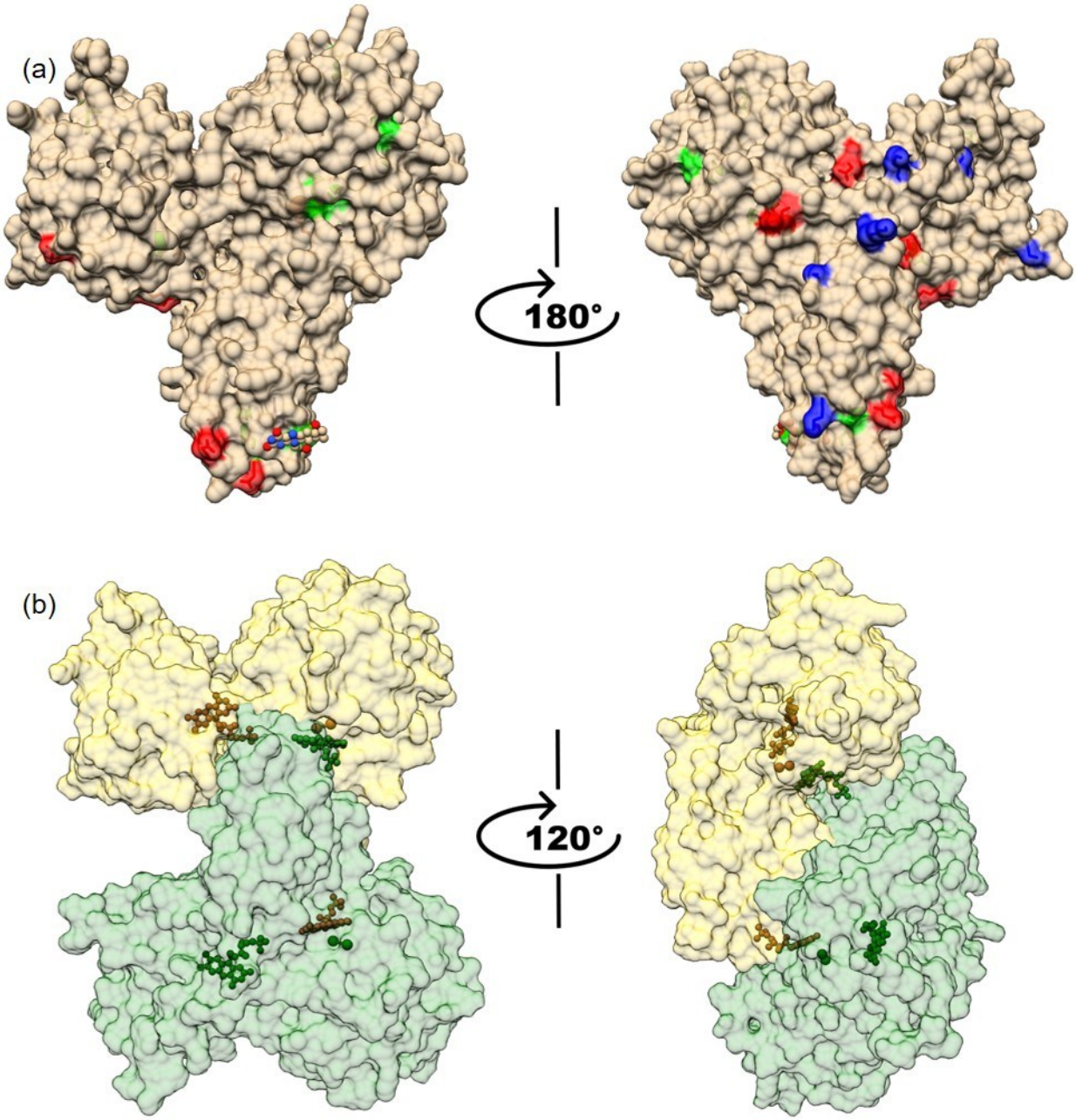

Figure S6. The solvent accessible surface of the intact Flv3 homodimers mapped using surface labeling. (**a**) Protein surface map of the Flv3 monomer shows GEE (modified sites, red) and DnsCl (modified sites, blue) labels incorporated into the native complex after a 15 min labeling reaction. Residues in green are sites where both labels were detected at later time points. Homology model of the dimer was generated in ClusPro using GEE/DnsCl labeled residues and predicted cofactor binding sites as spatial restraints for docking algorithm. The model in panel (**b**) was selected from 28 similar ClusPro generated dimer configurations based on acceptable distance constraints (less than 10 Å) between diiron and FMN cofactors and are in complete agreement with surface labeling results (Figure S2).

Table S9. Cofactor distances calculated from Flv3 homology model.

Cofactor 1	Atom 1	Cofactor 2	Atom 2	Distance (Å)
FMN	C2	**FMN**	N3	17.9
FMN	C2	**FMN**	N3	16.3
FMN	N5	**Fe**	Fe	4.2
FMN	C6	**Fe**	Fe	4.4
FMN	C6	**FMN**	C6	36.4
FMN	N5	**Fe**	Fe	39.7
Fe	Fe	**FMN**	C2	18.7
Fe	Fe	**FMN**	C2	18.9
FMN	C2	**FMN**	N10	46.5
FMN	C9	**FMN**	C9	47.4
FMN	N10	**NAD**	C2N	3.4
FMN	C6	**NAD**	C4N	4.1

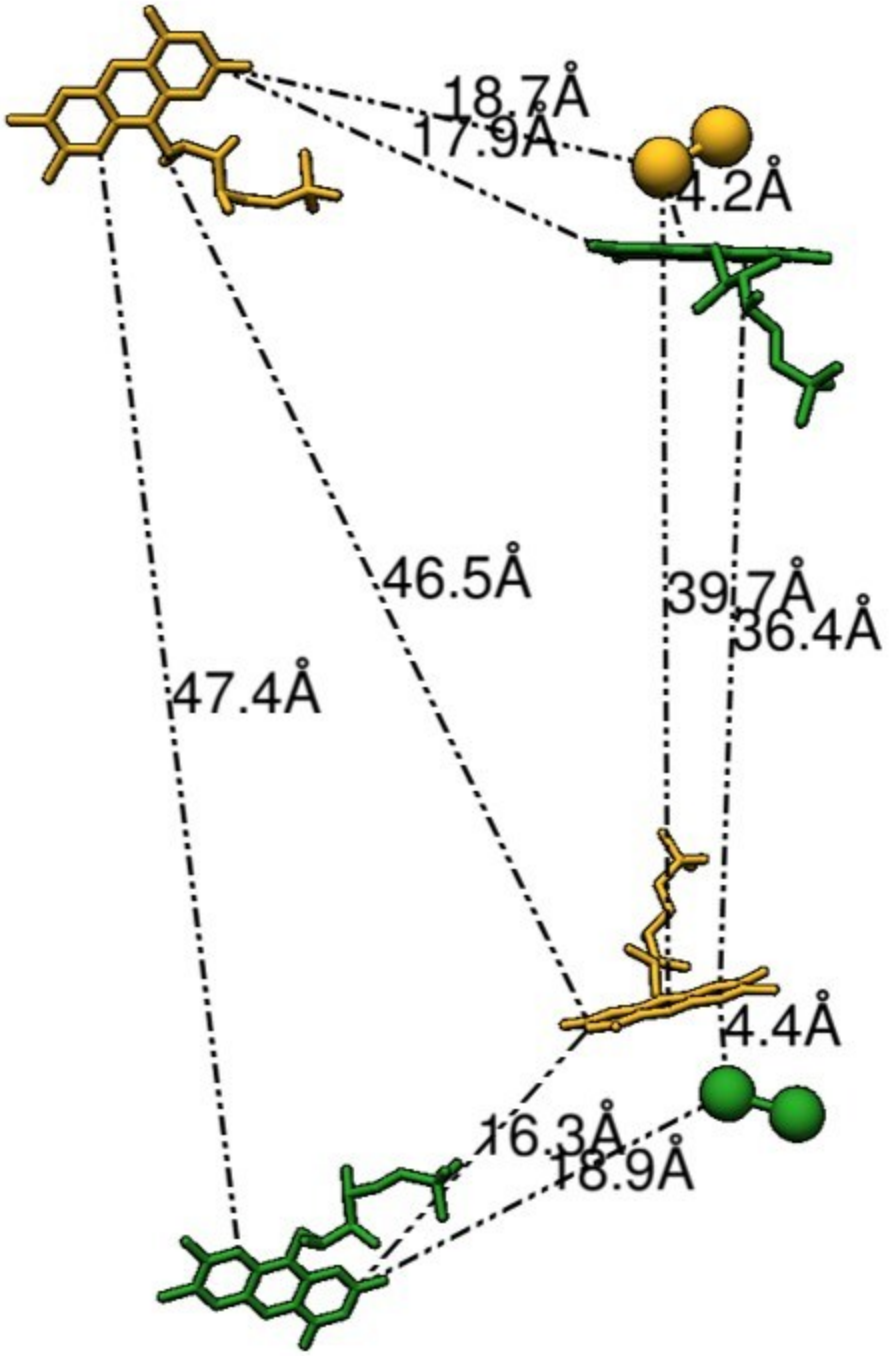

Figure S7. Model of the cofactor site distances in a Flv3 homodimer. Dotted lines show the calculated distances between flavin and diiron cofactors. Coloring indicates the cofactors that are common to each of the two monomers.

References

1. H. Rupp, K. Rao, D. Hall and R. Cammack, *Bioch. Biophys. Acta*, 1978, **537**, 255-269.